Monthly Notices
of the
ROYAL ASTRONOMICAL SOCIETY

Mon. Not. R. Astron. Soc. **423,** 2451–2463 (2012) doi:10.1111/j.1365-2966.2012.21051.x

The influence of fallback discs on the spectral and timing properties of neutron stars

T. Yan,[1⋆] R. Perna[1,2] and R. Soria[3]

[1]*Department of Astrophysical and Planetary Sciences, University of Colorado, Boulder, CO 80309, USA*
[2]*JILA, Boulder, CO 80309, USA*
[3]*International Centre for Radio Astronomy Research, Curtin University, GPO Box U1987, Perth, WA 6845, Australia*

Accepted 2012 April 3. Received 2012 March 19; in original form 2012 January 23

ABSTRACT

Fallback discs around neutron stars (NSs) are believed to be an expected outcome of supernova explosions. Here we investigate the consequences of such a common outcome for the timing and spectral properties of the associated NS population, using Monte Carlo population synthesis models. We find that the long-term torque exerted by the fallback disc can substantially influence the late-time period distribution, but with quantitative differences which depend on whether the initial spin distribution is dominated by slow or fast pulsars. For the latter, a single-peaked initial spin distribution becomes bimodal at later times. Timing ages tend to underestimate the real age of older pulsars, and overestimate the age of younger ones. Braking indices cluster in the range $1.5 \lesssim n \lesssim 3$ for slow-born pulsars, and $-0.5 \lesssim n \lesssim 5$ for fast-born pulsars, with the younger objects found predominantly below $n \lesssim 3$. Large values of n, while not common, are possible, and associated with torque transitions in the NS+disc system. The 0.1–10 keV thermal luminosity of the NS+disc system is found to be generally dominated by the disc emission at early times, $t \lesssim 10^3$ yr, but this declines faster than the thermal surface emission of the NS. Depending on the initial parameters, there can be occasional periods in which some NSs switch from the propeller to the accretion phase, increasing their luminosity up to the Eddington limit for $\sim 10^3$–10^4 years.

Key words: accretion, accretion discs – pulsars: general.

1 INTRODUCTION

Neutron stars (NSs) are born in supernova (SN) explosions. While the stellar core collapses, the envelope is ejected outwards. The ejected material carries angular momentum, due to the rotation of the progenitor star. If a fraction of the ejecta does not have enough energy to escape, it will form a fallback accretion disc around the collapsed core (Michel 1988; Chevalier 1989). Although a systematic and quantitative study of the fate of the ejected material following an SN explosion is still lacking, fallback discs around NSs have been invoked to explain a wide range of NS properties, such as enhanced X-ray luminosities in the anomalous X-ray pulsar (Chatterjee & Hernquist 2000; Chatterjee, Hernquist & Narayan 2000; Alpar 2001; Alpar, Ankay & Yazgan 2001), pulsar braking indices that suggest non-dipolar torques (Menou, Perna & Hernquist 2001a), pulsar jets (Blackman & Perna 2004; Blaschke, Grigorian & Voskresensky 2004) and discrepancies between the real (kinematic) pulsar ages and their characteristic ages $\tau = P/2\dot{P}$ (Marsden, Lingenfelter & Rothschild 2001a; Marsden et al. 2001b).

From an observational point of view, the search for fallback discs has been quite active in the last decade or so. Following up on the suggestion that fallback discs around NSs are brighter in the infrared (IR) and at longer wavelengths (Perna & Hernquist 2000; Perna, Hernquist & Narayan 2000), a number of isolated NSs have been imaged in those bands (Coe & Pightling 1998; Hulleman et al. 2000a; Hulleman, van Kerkwijk & Kulkarni 2000b; Kaplan, Kulkarni & Murray 2001; Israel et al. 2003; Mignani et al. 2007b; Wang, Kaplan & Chakrabarty 2007a; Wang, Kaspi & Higdon 2007b; Posselt et al. 2010). In particular, Wang, Chakrabarty & Kaplan (2006) reported the first direct detection of a fallback disc around an isolated NS, based on an IR excess which could be well modelled with emission from a passive, dusty disc. Evidence for IR excess has also been reported in other NS systems (Israel et al. 2003; Kaplan et al. 2009).

If fallback discs around NSs are indeed a ubiquitous phenomenon, they can substantially interfere with the spin evolution of the NS. This will affect estimates of the NS spin birth distribution based on the measured values of the period P and its derivative $\dot{P}$, and the simple assumption that the pulsar slow down is due to dipole radiation only. The distribution of NS spin births, which contains information on the physics of the SN explosion, has indeed been

⋆E-mail: ting.yan@colorado.edu

the subject of extensive investigation for several decades (Gunn & Ostriker 1970; Phinney & Blandford 1981; Srinivasan, Dwarakanath & Bhattacharya 1984; Lyne, Manchester & Taylor 1985; Narayan & Ostriker 1990; Arzoumanian, Chernoff & Cordes 2002; Faucher-Giguère & Kaspi 2006; Perna et al. 2008).

In this paper, we perform a statistical study of the spin evolution of NSs under the combined evolution resulting from dipole radiation losses and the interaction with a fallback disc. We aim at (a) assessing to what extent the inferred spin birth properties of pulsars can be influenced by the presence of fallback discs, (b) identifying observational properties that can help confirm/rule out a ubiquitous presence of fallback discs and (c) exploring whether fallback discs can help explain some currently puzzling pulsar observations.

Our paper is organized as follows. The coupled evolution of the disc and pulsar system is described in Section 2.1. Evolutionary tracks for several specific combinations of initial conditions are presented and discussed in Section 2.2 (timing properties) and Section 2.3 (luminosity). We present the statistical timing and luminosity properties of the pulsar population, derived via Monte Carlo simulations, in Section 3.1, while in Section 3.2 we further discuss the luminosity properties of the NS+disc system, and its differences from other astrophysical sources. We summarize and conclude in Section 4, highlighting puzzling pulsar observations which can be accounted for by the presence of fallback discs.

2 A MODEL OF FALLBACK ACCRETION

2.1 Time evolution of the accretion flow

We model the combined dipole/disc torque acting on the NS (rotating at angular velocity Ω) following the approach of Menou et al. (1999, see also Menou et al. 2001a):

$$I\dot{\Omega} = -\beta\Omega^3 + 2\dot{M}R_{\rm in}^2\Omega_{\rm K}(R_{\rm in})\left[1-\frac{\Omega}{\Omega_{\rm K}(R_{\rm in})}\right], \quad (1)$$

where $R_{\rm in}$ is the inner radius of the disc, $I = \frac{2}{5}M_{\rm NS}R_{\rm NS}^2$ is the moment of inertia of the NS, $\beta = B^2R_{\rm NS}^6/6c^3$ (assuming for simplicity an orthogonal rotator), $\dot{M}$ is the accretion rate and $\Omega_{\rm K}$ is the Keplerian angular velocity, both evaluated at $R_{\rm in}$. The first term in the right-hand side of equation (1) represents the torque due to dipole radiation losses, whereas the second term describes the torque exerted by the disc. At high accretion rates, the ram pressure of the accreting material causes the disc to penetrate inside the magnetosphere, up to an inner radius at which the magnetic pressure balances the ram pressure. This special location is called the magnetospheric radius, $R_{\rm m} = 2.55\times10^8\dot{M}_{16}^{-2/7}M_{\rm NS,1}^{-1/7}B_{12}^{4/7}$ cm.

If, at any point during the coupled NS+disc evolution, the magnetospheric radius, $R_{\rm m}$, formally exceeds the light cylinder radius, $R_{\rm lc}\equiv c/\Omega$, the field lines on the disc are no longer able to exert a significant pressure on the disc. On the other hand, the ram pressure of the material from the accreting disc continues to act. The disc is not able to penetrate inside $R_{\rm lc}$, because the magnetic pressure from the NS would then push it outwards. Therefore, when $R_{\rm m}$ becomes formally larger than $R_{\rm lc}$, we assume that the disc torque is applied at $R_{\rm lc}$. In summary, the inner disc radius is located at $R_{\rm in} = \min[R_{\rm m}, R_{\rm lc}]$.

Inspection of equation (1) shows that, at any given time, if $\Omega < \Omega_{\rm K}(R_{\rm in})$, the disc exerts a positive torque, which, if dominant over the dipole component, would make the pulsar spin up and accrete. On the other hand, if $\Omega > \Omega_{\rm K}(R_{\rm in})$, material from the disc is stopped by the centrifugal barrier (Illarionov & Sunyaev 1975), and the disc contributes to further spin down the pulsar.

Formation of the fallback disc ensues as material from the stellar envelope is thrown out at large distances during the SN explosion; the fraction of this material which remains bound falls back, and circularizes on to Keplerian orbits corresponding to their original specific angular momentum (Chevalier 1989; MacFadyen et al. 2001; see also Perna & MacFadyen 2010, for an exploration of different angular momenta distributions in collapsing stars).

Once the initial disc has been formed, its subsequent evolution can be modelled following the results of the numerical simulations of Cannizzo, Lee & Goodman (1990). They showed that the accretion rate in the debris disc follows the evolution

$$\dot{M}(t) = \begin{cases} \dot{M}_0, & \text{for } 0 < t < t_0, \\ \dot{M}_0\,(t/t_0)^{-\alpha}, & \text{for } t > t_0, \end{cases} \quad (2)$$

where $\dot{M}_0$ is the accretion rate during an initial plateau phase lasting a time-scale t_0. Menou, Perna & Hernquist (2001b) estimated the time-scale of the transient accretion phase to be of the order of

$$t_0 = \frac{R^2\Omega_{\rm K}}{\alpha' c_{\rm s}^2} \approx 6.6\times10^{-5}(T_{\rm c,6})^{-1}R_{\rm d,8}^{1/2}(t_0)\ {\rm yr}, \quad (3)$$

where $c_{\rm s}$ is the sound speed, α' the viscosity parameter, $R_{\rm d,8}(t_0)$ the initial disc radius in units of 10^8 cm, and $T_{\rm c,6}$ a typical disc temperature during the early phases, in units of 10^6 K. The index α of the power-law decay was found to be $\approx$19/16. A similar behaviour, i.e. a plateau followed by a power-law decline, was also found in the simulations by MacFadyen, Woosley & Heger (2001), although with $\alpha \approx 5/3$. Here, we adopt $\alpha = 19/16$ for our model.

For an estimate of the expected range of values of the initial accretion rate, we rely on results of numerical simulations of massive star collapse and subsequent fallback on to the compact object. Mineshige et al. (1997) found that the fallback material accretes towards the central object with a supercritical accretion rate, exceeding the Eddington limit by at least a factor of 10^6. The simulations of MacFadyen et al. (2001), for the case of a $25\,{\rm M}_\odot$ star, yield $\dot{M}_0 \sim 10^{27}$–$10^{29}\,{\rm g\,s^{-1}}$. More recently, fallback in SNe was studied by Zhang, Woosley & Heger (2008) for a wide range of masses, and different metallicities and explosion energies. The full hydrodynamical study in one representative case yielded initial accretion rates of $\sim10^{29}\,{\rm erg\,s^{-1}}$. An analysis of SN 1987A (Chevalier 1989) showed that the accretion rate at the time of the reverse shock (7×10^3 s) is $2.2\times10^{28}\,{\rm g\,s^{-1}}$. In general, when considering a distribution of NSs, a distribution of initial[1] accretion rates is expected, as this depends on the angular momentum of the progenitor star, its mass and the energetics of the explosion. In our work, to be broadly consistent with the result of previous numerical work, as well as with that of previous semi-analytical investigations which used fallback discs, we select the initial accretion rate $\dot{M}_0$ to be distributed log-uniformly from 10^{25} to $10^{28}\,{\rm g\,s^{-1}}$. However, with these values, the mass accretion inflow at early times would be highly supercritical; that is, it would produce a highly super-Eddington luminosity if all the inflowing matter was efficiently accreted through the disc and on to the NS. The classical Eddington limit for an NS, $L_{\rm Edd} = 1.3\times10^{38}(M_{\rm NS}/{\rm M}_\odot) \approx 2\times10^{38}\,{\rm erg\,s^{-1}}$, requires only accretion rates $\dot{M} \sim 10^{18}\,{\rm g\,s^{-1}}$, for a radiatively efficient flow.

[1] Note that here we speak of 'initial' disc accretion rate as if the disc had been formed instantaneously, since the time-scale of disc formation, of the order of the dynamical time-scale of collapse of the star envelope (tens of seconds), is much shorter than the time-scale (thousands of years) of interest here for the fallback disc to affect the pulsar timing evolution.

Faced with a highly supercritical accretion flow at the outer boundary, an accreting system has only two options (Poutanen et al. 2007): it can accrete most of it in a radiatively inefficient way (e.g. the 'Polish donut' or 'slim disc' classes of accretion flows; Abramowicz et al. 1988; Watarai et al. 2000); or it can spend most of the accretion power to blow away the excess infalling mass, in a radiatively driven wind (Shakura & Sunyaev 1973). For an accreting black hole, observational data and hydrodynamical simulations suggest that the physical situation is a combination of both effects (Ohsuga & Mineshige 2011). For an accreting NS, the presence of a hard surface prevents advective solutions: the excess gravitational energy released during accretion cannot be carried through a horizon and will always be dissipated, eventually. Therefore, in our model we assume that supercritical inflows on a young NS will lead to massive outflows. Following Shakura & Sunyaev (1973) and Poutanen et al. (2007), we assume that only $\dot{M} \approx \dot{M}_{\rm Edd} \equiv L_{\rm Edd}/0.1c^2$ reaches the inner edge of the accretion disc (from where it can then plunge on to the NS), regardless of the mass supply at the outer disc, and that the accretion rate through each radius decreases linearly, $\dot{M} \sim R$, because of radiation-driven wind losses. Thus, we parametrize the radial dependence of the mass flow in the disc at a fixed time as

$$\dot{M}(R) = \dot{M}(R_{\rm in}) + [\dot{M}(R_{\rm out}) - \dot{M}(R_{\rm in})]\frac{R - R_{\rm in}}{R_{\rm out} - R_{\rm in}}\,, \qquad (4)$$

where $\dot{M}(R_{\rm out}, t) \equiv \dot{M}(R_{\rm out}, t_0)$, for $0 < t < t_0$, and $\dot{M}(R_{\rm out}, t_0)\,(t/t_0)^{-\alpha}$, for $t > t_0$, is the rate of fallback mass inflow at the outer boundary, and $\dot{M}(R_{\rm in}, t) = \min\left[\dot{M}_{\rm Edd}, \dot{M}(R_{\rm out}, t)\right]$. In the rest of this paper, for clarity, we shall use the term 'accretion rate' when referring to $\dot{M}(R_{\rm in})$ (what is actually accreted through the whole disc), and 'inflow rate' for $\dot{M}(R)$ at larger radii, most of which is lost in the outflow at early epochs. (See also Kuncic & Bicknell 2007, for analytical modelling of accretion discs with a power-law scaling of the inflow rate $\dot{M}(R) \sim R^b$.) Recalling the definition of magnetospheric radius $R_{\rm m}$, it is possible that at early times, when the accretion rate is near Eddington, $R_{\rm m} < R_{\rm NS}$: in that case the disc extends all the way to the NS surface, and we assume the disc torque to be $\dot{M}_{\rm Edd} R_{\rm NS}^2 \Omega_{\rm K}(R_{\rm NS})$.

At intermediate epochs, when $\dot{M}(R_{\rm out}, t) \approx \dot{M}(R_{\rm in}, t) < \dot{M}_{\rm Edd}$, the wind subsides, and the inflow rate becomes constant throughout the disc and equal to the accretion rate at the inner edge of the disc. Finally, at late times, the accretion rate declines further, until it reaches a value comparable to what is expected from accretion from the interstellar medium. From that epoch onwards, we take $\dot{M}$ to be constant, $\dot{M} \sim 2 \times 10^{11}\,{\rm g\,s^{-1}}$, equal to the Bondi accretion rate (Bondi 1952; Frank, King & Raine 2002) for a medium with characteristic temperature $kT \sim 10^3$ keV and number density $n \sim 1\,{\rm cm^{-3}}$. Although the precise value of the Bondi accretion rate in a low-density medium depends on the details of the accretion mode (Blaes & Madau 1993; Popov et al. 2000; Perna et al. 2003), our results, which focus on moderately young pulsars, are not very sensitive to the choice of the late-time asymptotic value.

2.2 Time evolution of the pulsar timing properties

As discussed above, at any time during the pulsar evolution, either the disc can contribute to spinning down the pulsar even more (with respect to the dipole term alone), or it can offset the dipole term and spin the pulsar up. Fig. 1 shows, for several values of the accretion rate, the *P*–*B* parameter space in which the pulsar spins up (down).

At late times, the torque may disappear if the disc becomes neutral, viscous dissipation drops and accretion stops. Menou et al. (2001b) estimated a neutralization time-scale

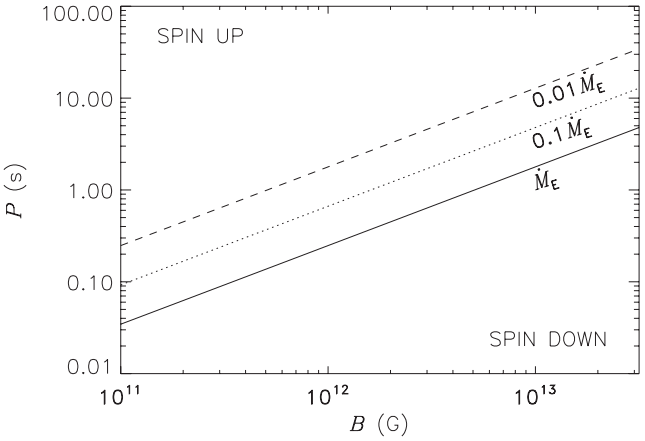

Figure 1. Range of the *P*–*B* parameter space in which the pulsar is either spinning up or down, owing to the combined effect of dipole radiation losses and torque by a disc. For each value of the accretion rate at the magnetospheric radius, the region above its corresponding curve represents the parameter space where the pulsar is spun up, while the region below represents spin-down conditions.

$$t_{\rm n} = \left[\frac{R_{\rm d,10}^3(t_0)}{\dot{M}(t_0)/10^{16}\,{\rm g\,s^{-1}}}\right]^{1/2.75} t_0, \qquad (5)$$

where $R_{\rm d,10}$ is the disc radius in units of 10^{10} cm. The possible onset of a transition to a phase of 'dead' disc is rather uncertain, as it depends on the nature of viscosity; opacity (and hence disc composition) also plays an important role, as well as the disc size (Menou et al. 2001b). Furthermore, it has been pointed out that irradiation by the pulsar is likely to keep the disc ionized and continue the mass inflow (Alpar et al. 2001). Here, to avoid introducing highly uncertain parametrizations, we assume that the disc is active throughout the active lifetime of the pulsar. If the disc were to become dead at some point, from that time on the pulsar would simply continue its evolution as an isolated pulsar, spinning down by dipole radiation losses alone (neglecting gravitational energy losses and other secondary effects).

The birth distribution of surface magnetic fields and spin periods has been the subject of numerous studies. Usually, a log-Gaussian distribution is assumed for both. For the *B* field distribution, there is now a general consensus about the initial parameters; following Arzoumanian et al. (2002), we take

$$\langle \log B_0({\rm G}) \rangle = 12.35, \quad \sigma_{\log B_0} = 0.4\,. \qquad (6)$$

Whether accretion leads to field decay and the time-scale over which the magnetic field re-emerges are still unsettled issues, especially with regards to quantitative details. Several papers have been devoted to this topic (e.g. Geppert, Page & Zannias 1999; Cumming, Zweibel & Bildsten 2001), and the coupled evolution between an NS with a fallback disc and a field gradually buried by the disc accretion has been studied by Liu & Li (2009), using an empirical expression for *B*-field decay presented by Shibazaki et al. (1989), $B = B_0/(1 + \Delta M/m_B)$, where ΔM is the accreted mass and m_B is a mass normalization constant with typical values between $\sim 10^{-5}$ and $10^{-4}\,{\rm M_\odot}$. The resulting evolutionary tracks for the periods of the NS studied were found to be very model dependent, with the magnitude of the effect depending on both the initial *B* field and the disc properties. In the current work, to avoid results dependent on a rather uncertain parametrization, we consider the case of negligible

field burying. We stress that our investigation is aimed at capturing features of pulsar properties which could be attributed to NS–disc interaction, but we do not make any attempt to quantitatively model data.

For the birth period distribution, on the other hand, there is a widely different range of values inferred by different investigations: from a distribution peaking around a few ms (Arzoumanian et al. 2002),

$$\langle \log P_0(\mathrm{s}) \rangle = -2.3, \quad \sigma_{\log P_0} > 0.2, \tag{7}$$

to one peaking at several hundred ms (Faucher-Giguère & Kaspi 2006),

$$\langle \log P_0(\mathrm{s}) \rangle = -0.5, \quad \sigma_{\log P_0} = 0.2. \tag{8}$$

A lower limit of several tens of ms was derived from the scarcity of bright X-ray pulsars associated with historical SNe (Perna et al. 2008). It should be pointed out, however, that all those investigations assumed that pulsar evolution occurs with no contribution from fallback torques. Therefore, we use them here as an initial reference point to study the effect that hypothetical fallback discs would have on the pulsar evolution, at a statistical level. We take an initial spin distribution that encompasses the broad range of values inferred by previous investigations. In fact, one of the goals of our study is to uncover differences in the effect that a torque by a disc has on NSs born with fast and slow spins. However, we do need to note that it is possible that discs might be much more common around slow-born NSs than fast-born NSs, since the rotational energy of the latter can rapidly disrupt the disc (Ekşi, Hernquist & Narayan 2005).

The presence of a fallback disc torque, in addition to the dipole contribution, can be tested with measurements of the braking index, an observable quantity defined as

$$n = \frac{\Omega\ddot{\Omega}}{\dot{\Omega}^2}, \tag{9}$$

and of the timing age,

$$\tau = \frac{P}{2\dot{P}}, \tag{10}$$

where $P = 2\pi/\Omega$. If the primary source of spin-down is due to dipole radiation losses, then $n = 3$, and the timing age of the pulsar is equal to the real age, if $P_0 \ll P$.

Fig. 2 shows the time evolution of the braking index, timing age and the absolute magnitude of the dipole and disc torques, for four representative pulsars, suitably chosen to represent a wide range of initial birth parameters. For a fixed initial B field strength B_0 (defined in equation 6), we consider the time evolution for a typical slow-born ($P_0^{\rm s} = 300$ ms) and fast-born ($P_0^{\rm f} = 5$ ms) pulsar, with an initial fallback rate either at the maximum ($\dot{M}_{0,\rm MAX} = 10^{28}$ g s^{-1}) or at the minimum value ($\dot{M}_{0,\rm MIN} = 10^{25}$ g s^{-1}) of the assumed distribution. In order to compute the evolutionary tracks shown in Fig. 2 by means of equations (9) and (10), we use equation (1) to evaluate $\dot{\Omega}$, from which $\ddot{\Omega}$ and Ω are derived through numerical differentiation and numerical integration, respectively. For the latter, the initial condition is $\Omega(t = 0) = 2\pi/P_0$, with $P_0 = P_0^{\rm f}$ or $P_0 = P_0^{\rm s}$ depending on the case. Note that in equation (1) $\dot{M}$ represents the accretion rate at the inner disc boundary, i.e. $\dot{M}(R_{\rm in}) = \min\left[\dot{M}_{\rm Edd}, \dot{M}(R_{\rm out}, t)\right]$, where, recalling from Section 2.1, $\dot{M}(R_{\rm out}, t) \equiv \dot{M}(R_{\rm out}, t_0)$ for $0 < t < t_0$ and $\dot{M}(R_{\rm out}, t_0)\,(t/t_0)^{-\alpha}$ for $t > t_0$. For each combination of system parameters B_0, P_0, $\dot{M}(R_{\rm out}, t_0)$, the timing evolution of the NS driven by the coupled disc+dipole torques is therefore uniquely determined.

The result of our calculations is that the disc torque is always negative, that is $\Omega > \Omega_{\rm K}$ (corresponding to a spin-down/propeller regime), except for a few brief phases when the accretion rate is very high and $\Omega < \Omega_{\rm K}$ (corresponding to a spin-up/accretor regime, see also Section 2.3). The absolute magnitudes of the disc and dipole torques (dotted and dashed lines, respectively) are plotted in Fig. 2; the short epochs in which the sign of the disc torque is positive are plotted with red dots (Fig. 2, left-hand panels). The presence of significant (and variable) disc torques causes the braking index to vary. More generally, n goes through discontinuities caused by transitions between disc-driven spin-up and spin-down phases, between phases of constant accretion rate and power-law decay, and when the location of the inner radius of the disc switches between $R_{\rm m}$ and $R_{\rm lc}$. In between those rapid transitions, the complex behaviour of the braking index is mostly determined by the non-linear coupling between NS spin, inner radius of the disc and accretion rate. In particular, for fast pulsars, the dipole torque largely dominates over the disc torque at early times, while the latter dominates at later times. Instead, for slow pulsars, the disc torque is larger than the dipole component at almost all times. Both slow and fast pulsars have a roughly constant braking index during the first few 10^3 yr, corresponding to the epoch when $\dot{M}(R_{\rm out}) \approx$ constant and $\dot{M}(R_{\rm in}) \approx \dot{M}_{\rm Edd}$. However, the index is exactly $n = 3$ for (dipole-dominated) fast pulsars, while it is $n \approx \Omega/[\Omega - \Omega_{\rm K}(R_{\rm in})]$ for (disc-dominated) slow pulsars (from equation 1). The constancy of n in the regime of disc-dominated torque is expected as long as both $\dot{M}(R_{\rm in})$ and Ω are roughly constant.

After the first constant phase, there are three types of discontinuity that can occur on the braking index. The most dramatic is the transition between spin-down and spin-up phases, which formally results in an infinite value for n. These reversals correspond to switches between NS surface accretion and propeller phases. In our simulations, they happen only at the high end of the initial fallback rate (Fig. 2, left-hand panels); for lower inflow rates, the system remains in the propeller phase all the time. Another discontinuity is caused by the transition of the accretion rate at the inner disc radius from the early-time Eddington rate to a power-law decay. This discontinuity in $\ddot{\Omega}$ will appear only if the disc torque dominates over the dipole torque at the time when $\dot{M}$ undergoes the transition. Lastly, as discussed earlier, if, at any point during the pulsar evolution, $R_{\rm m}$ becomes formally larger than $R_{\rm lc}$, the magnetic pressure of the pulsar is not able to push the disc further out, and hence the inner disc boundary tracks $R_{\rm lc}$. Since the time dependence of $R_{\rm m}$ [modulated by $\dot{M}(R_{\rm in})$] and that of $R_{\rm lc}$ (dictated by Ω) are different, these two radii increase at different rates with time; hence, the inner radius of the disc, $R_{\rm in}$, can transition between $R_{\rm m}$ and $R_{\rm lc}$ (or vice versa) during the coupled NS/disc evolution. Any time there is such a transition, the torque in the right-hand side equation (1) changes functional form with time, and hence so does $\dot{\Omega}$.

We need to remark that our semi-analytical treatment of the torque (equation 1) naturally leads to the transitions between the various phases of the coupled disc/NS evolution to be abrupt. In reality, it is likely that at least some of these transitions will be smoother. However, we also note that sharp transitions in the period (and hence discontinuities in its derivative) are often observed in binary systems, where the NS dynamics is known to be driven by the disc (see Bildsten et al. 1997, for a comprehensive study).

An important feature in the evolution of the braking index is a period of time during which $n \approx 1$. This phase sets in when the disc torque begins to dominate over the pulsar torque, and at the same time $\Omega \gg \Omega_{\rm K}$. Then, the NS spin is driven by the equation $I\dot{\Omega} \approx -2\dot{M}R_{\rm m}^2\Omega$, and the braking index can be written as $n \approx 1 + (t/t_*)^{(3/7\alpha\ -1)}$, where t_* is a constant dependent on a combination of the system parameters. For our choice of $\alpha = 19/16$, $n \approx 1$ if

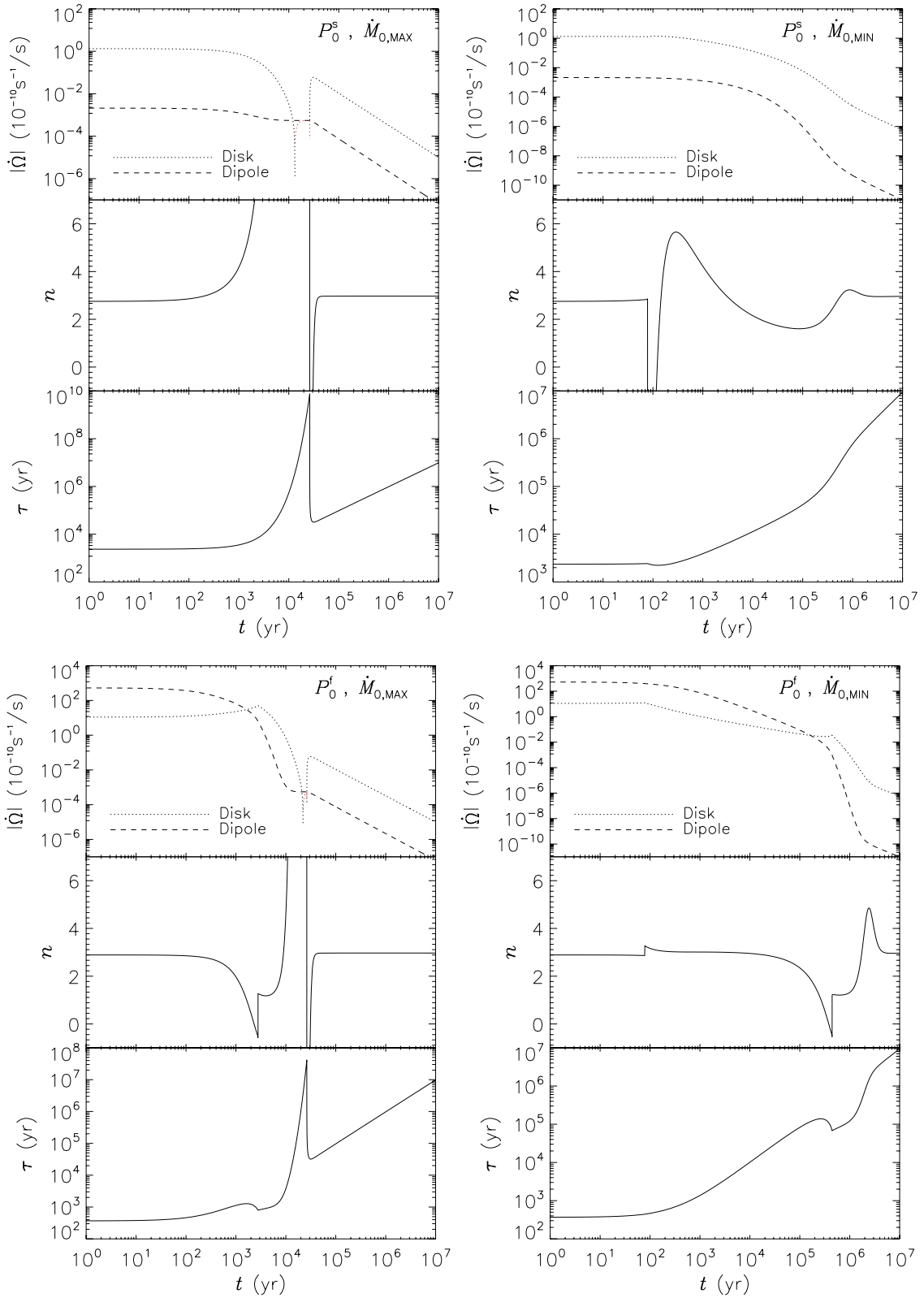

Figure 2. Time evolution of the dipole and disc components of the spin-down rate $|\dot{\Omega}|$, of the braking index n and of the timing age τ, for slow-born ($P_0^{\rm s} = 300\,{\rm ms}$; top panels) and fast-born ($P_0^{\rm f} = 5\,{\rm ms}$; bottom panels) pulsars, starting with either a high ($\dot{M}_{0,\rm MAX} = 10^{28}\,{\rm g\,s^{-1}}$; left-hand panels) or a low ($\dot{M}_{0,\rm MIN} = 10^{25}\,{\rm g\,s^{-1}}$; right-hand panels) fallback inflow rate at the outer boundary of the disc. $\dot{\Omega}$ is always negative (spin-down), except for occasional brief disc spin-up phases, marked by red dots (left-hand panels). For the breaking index, we note a characteristic $n \approx 1$ transitional phase that happens only in fast-born pulsars (bottom panels).

$t \gg t_*$, and the two conditions above are satisfied. In our simulations, we find that the (short-lived) $n \approx 1$ phase is a telltale feature of fast-born pulsars, but is not seen in slow-born pulsars, because the latter do not go through a phase with $\Omega \gg \Omega_{\rm K}$.

At late times, we find that the disc torque dominates over the dipole torque both for the slow and the fast pulsars; Ω and $\Omega_{\rm K}$ track each other, and the torque evolution is approximately given by $I\dot{\Omega} \approx 2\dot{M}R_{\rm m}^2\Omega_{\rm K}(R_{\rm m})[1-\Omega/\Omega_{\rm K}(R_{\rm m})]$. The precise time evolution of the torque depends on the index α of the accretion rate. For $\alpha = 19/16$, the time dependence is close to $\propto t^{-1.5}$, like in the case of a dipole-dominated torque, and $n \approx 3$. Larger values of α would yield somewhat smaller values of n at late times.

2.3 Luminosity evolution

The luminosity of an NS with a fallback disc is given by the sum of two terms: a thermal component due to the hot surface of the NS and another thermal component (multiblackbody) due to radiatively efficient viscous dissipation in the accretion flow. The ultimate source of power is internal heat for the first term, and for the second term it is the gravitational potential drop of the fallback matter. In turn, the accretion power can be split into separate contributions from the accretion disc, from the boundary layer and from the NS surface. Furthermore, when the disc does not penetrate inside the light cylinder (i.e. when $R_{\rm in} = R_{\rm lc}$), the pulsar mechanism is likely to operate and then magnetospheric emission, powered by the pulsar spin-down, is also present.

More in detail, the various emission components are as follows.

(i) *NS emission*. The main component, always present with or without a disc, is the surface emission of the NS due to its internal cooling. We model the resulting X-ray luminosity using the standard cooling model of Blaschke et al. (2004), for a $1.4\,{\rm M}_\odot$ NS, with radius of 10 km. Furthermore, as discussed above, there can be periods during the coupled NS/disc evolution when the pulsar mechanism is able to operate, converting a fraction of the spin power of the NS into non-thermal X-ray radiation. Observationally, a correlation between the spin power $\dot{E}_{\rm rot}$ and the 2–10 keV luminosity has been investigated in numerous studies (e.g. Saito et al. 1997; Possenti et al. 2002; Kargaltsev & Pavlov 2008). In particular, Possenti et al. (2002) derive the best-fitting relation

$$\log L_{\rm X,[2-10]} = 1.34 \log \dot{E}_{\rm rot} - 15.34\,, \tag{11}$$

with $L_{\rm X}$ and $\dot{E}_{\rm rot} = I\Omega\dot{\Omega}$ in CGS units. When present, such a component would manifest itself as a power-law spectrum of photon index $\Gamma \approx 2$.

In this work, since we are specifically interested in the properties of fallback discs and their effects on NSs, we compute in detail the various components of the emission due to the disc itself (viscous dissipation, irradiation) and its interaction with the NS (boundary layer, accretion). However, since the surface emission of the NS cannot be hidden, we also include this contribution for reference and comparison to the components above. For the magnetospheric component, on the other hand, we will limit ourselves to a discussion, since the presence of this component depends on the location of $R_{\rm in}$ at a given time, and its magnitude is determined by the timing parameters of the NS at that time.

(ii) *Surface accretion luminosity*. This term is given by the potential and kinetic energy released by matter falling from the magnetospheric radius to the surface of the NS; hence, in the Newtonian approximation it is

$$L_{\rm acc} = GM\dot{M}\left(\frac{1}{R_{\rm NS}} - \frac{1}{R_{\rm in}}\right) + \frac{1}{2}\Omega^2\left(R_{\rm in}^2 - R_{\rm NS}^2\right)\,. \tag{12}$$

For the characteristic radius of an NS ($\approx$10 km), the effective blackbody temperature of the surface accretion luminosity spans the soft X-ray band, between $\sim$0.1 and $\sim$2 keV, for a large range of luminosities, from those characteristic of Bondi accretion from the interstellar medium (Zampieri et al. 1995) up to the Eddington luminosity. It is important to note that this component is present only when $R_{\rm in} = R_{\rm m} < R_{\rm co}$, where $R_{\rm co}$ is the corotation radius, i.e. the radius at which the Keplerian rotation of the material is equal to the rotation rate of the star Ω [condition equivalent to $\Omega < \Omega_{\rm K}(R_{\rm m})$]. Otherwise, the pulsar is found in the propeller phase, accretion is inhibited, and the corresponding luminosity contribution can be considered negligible.

(iii) *Boundary layer luminosity*. This contribution is due to the release of energy in the boundary layer between the Keplerian disc and the magnetosphere. We estimate the boundary layer luminosity with the following argument, following Perna et al. (2006). We adopt the 'elasticity parameter' β, which is a measure of how efficiently the kinetic energy of the NS is converted into kinetic energy of ejected matter through the magnetosphere–disc interaction (Ekşi et al. 2005). In the limit of a completely anelastic propeller ($\beta = 0$), the magnetosphere forces matter to corotate with it during both the accretion and the propeller regime. On the other hand, in the limit of a completely elastic propeller ($\beta = 1$), matter is slowed down in the boundary layer; this term is present only during the propeller phase. For a generic value for the elasticity parameter, the luminosity of the boundary layer can be written as

$$L_{\rm BL} = \begin{cases} \dfrac{\dot{M}}{4\pi}\left[R_{\rm m}^2\left(\Omega_{\rm K}^2 - \Omega^2\right)\right] & \text{for } R_{\rm m} < R_{\rm co} \\ \dfrac{\dot{M}}{4\pi}(1-\beta)\left[R_{\rm m}^2\left(\Omega^2 - \Omega_{\rm K}^2\right)\right] & \text{for } R_{\rm m} \geq R_{\rm co}\,. \end{cases} \tag{13}$$

Given the uncertainties in the parameter β, here we adopt $\beta = 1$, which yields a lower limit to the attainable boundary layer luminosity during the lifetime of the NS.

(iv) *Disc luminosity*. This contribution is clearly present in both the accretion and the propeller regime. For an optically thick, geometrically thin disc model (Shakura & Sunyaev 1973; Frank et al. 2002), the luminosity in the $[\nu_1, \nu_2]$ frequency band is given by an integration over radial annuli:

$$L_{[\nu_1-\nu_2]} = 2\pi\int_{\nu_1}^{\nu_2}{\rm d}\nu\,\frac{h\nu^3}{c^2}\int_{R_{\rm in}}^{R_{\rm out}}\frac{R\,{\rm d}R}{{\rm e}^{h\nu/kT(R)}-1}\,, \tag{14}$$

each producing a blackbody spectrum at a temperature

$$T(R) = \left(\frac{3GM_{\rm NS}\dot{M}(R)}{8\pi R^3\sigma}\right)^{1/4}\left[1-\left(\frac{R_{\rm in}}{R}\right)^{1/2}\right]^{1/4}\,. \tag{15}$$

Besides emission due to internal energy dissipation, the disc can brighten up also as a result of reradiation of X-rays impinging from the central object. We use Vrtilek et al.'s (1990) analytical expression for the effective temperature of an irradiated disc, under the assumption that the disc height $h \propto r^n$ and irradiation is the dominant form of heating. If particles in the disc are in Keplerian motion, then $n = 9/7$, and the temperature profile is given by

$$T_{\rm X}(r) = \left[f\frac{\sqrt{k_{\rm B}/\mu m_{\rm H}}L_{\rm X}\omega}{14\pi\sigma GM}\right]^{2/7} \simeq 2.32\times10^4\left(\frac{f}{0.5}\right)^{2/7}\left(\frac{L_{\rm X}}{L_{\rm E}}\right)^{2/7}\left(\frac{{\rm R}_\odot}{r}\right)^{3/7}\,{\rm K}, \tag{16}$$

where L_X is the X-ray luminosity of the central source, and f parametrizes the uncertainty in the disc structure and albedo. To a first approximation, the total luminosity in the $[\nu_1, \nu_2]$ band is the sum of the viscous dissipation and reradiation components; the former dominates at small radii, while the latter dominates in the outer disc.

Recall that we are not assuming a constant $\dot{M}$ throughout the disc. As we discussed in Section 2.1, at earlier times $\dot{M}(R) \sim R$ because of wind losses. Therefore, during the early supercritical accretion phase, the temperature profile in the inner disc is $T(R) \sim R^{-1/2}$, flatter than the standard disc blackbody profile, which scales as $R^{-3/4}$. Our choice of accepting an Eddington-limited accretion rate at the innermost disc radius and a much higher mass inflow rate at the outer boundary implies that the integrated disc luminosity may exceed $L_{\rm Edd}$ at early times. However, it is easy to see that for $\dot{M}(R) \sim R$, this excess is only a logarithmic function of $\dot{M}(R_{\rm out})/\dot{M}_{\rm Edd}$. This is a restatement of the well-known result that $L_{\rm disc} \approx [1 + \ln(\dot{M}/\dot{M}_{\rm Edd})]$ during super-Eddington accretion (Shakura & Sunyaev 1973; Frank et al. 2002). In our case, the highest possible inflow rate at the outer radius considered in our model, $\dot{M}(R_{\rm out})/\dot{M}_{\rm Edd} \sim 10^{10}$, would lead to a bolometric disc luminosity $\sim 20\, L_{\rm Edd}$, at least for the initial transient phase (or less, if $R_{\rm m} \gg 10$ km). We accept this possibility of transient super-Eddington luminosity as we are modelling a situation characterized by massive outflows rather than a steady-state solution. A more complex modelling of the accretion flow in that situation with a slim disc rather than a standard disc plus outflow approximation is beyond the scope of this work.

We begin by exploring the relative magnitude of the various components of the luminosity as a function of NS age, for a few representative combinations of NS and disc parameters. In particular, for the same choice of initial NS spin and disc accretion rate as in Fig. 2, we consider the time evolution of the surface accretion, boundary layer and the disc luminosity in the 0.1–10 keV, the 3–4 μm and in the 80–120 GHz bands. In the IR and the mm band, we compute only the disc luminosity, since the pulsar contribution in these bands is not well known. For comparison, we also show the timing evolution of the NS thermal emission in 0.1–10 keV. We assume an outer disc radius[2] $R_{\rm out} = 1000\, R_{\rm NS}$, and a face-on geometry. Hence, the predicted luminosities represent upper limits for discs with generic inclinations with respect to the observer line of sight.

Fig. 3 shows the evolutionary path of the various components of the luminosity, for the four combinations $\{\dot{M}_{0,\rm max}, P_0^{\rm f}\}$, $\{\dot{M}_{0,\rm max}, P_0^{\rm s}\}$, $\{\dot{M}_{0,\rm min}, P_0^{\rm f}\}$ and $\{\dot{M}_{0,\rm min}, P_0^{\rm s}\}$, where $\dot{M}_{0,\rm max} = 10^{28}\,{\rm g\,s^{-1}}$ and $\dot{M}_{0,\rm min} = 10^{25}\,{\rm g\,s^{-1}}$. We suggest the following physical interpretation of these results. At the low end of the initial fallback rate, the NS will never be found in an accretion phase; hence, both the surface accretion and the boundary layer luminosities will always be negligible. In the

[2] In reality, the outer radius of the disc is expected to be an increasing function of time. Modelling this in detail is, however, beyond the scope of our paper, since the magnitude of the disc torque depends only on the location of the inner boundary of the disc. The X-ray and IR luminosity of the disc is also not very sensitive to the outer radius (unless very small), since it is produced relatively close to $R_{\rm m}$, while the mm luminosity is more sensitive to the exact value of $R_{\rm out}$ (see e.g. Posselt et al. 2010).

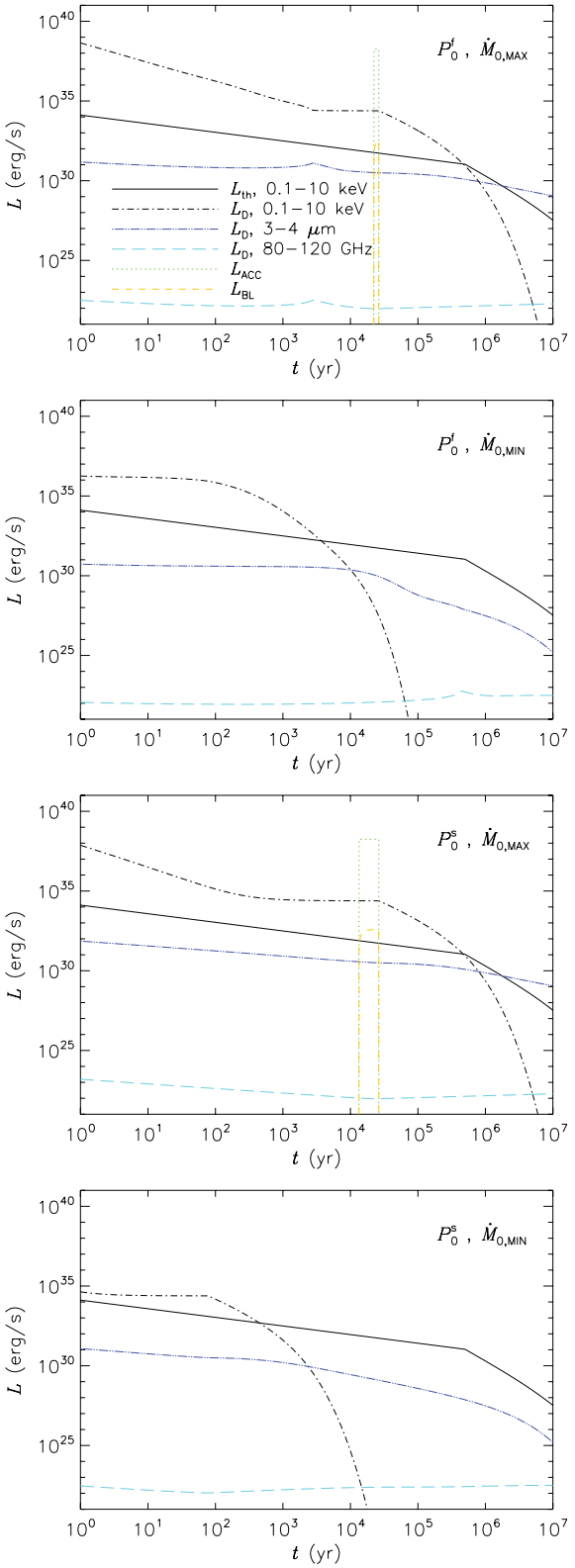

Figure 3. Time evolution of the various components of the NS+disc luminosity, for fast-born ($P_0^{\rm f} = 5$ ms) and slow-born ($P_0^{\rm s} = 300$ ms) pulsars, accreting at $t = 0$ with either a high ($\dot{M}_{0,\rm max} = 10^{28}\,{\rm g\,s^{-1}}$) or a low ($\dot{M}_{0,\rm min} = 10^{25}\,{\rm g\,s^{-1}}$) inflow rate. $L_{\rm th}$ indicates the thermal surface emission of the NS.

0.1–10 keV band, it is interesting to note that the disc luminosity exceeds that from the NS surface under all choices of parameters, for an age $t \lesssim 10^3$ yr. The higher the accretion rate, the longer is the time over which the disc luminosity exceeds that of the NS (compare panels labelled $\dot{M}_{0,\rm MAX}$ with those labelled $\dot{M}_{0,\rm MIN}$ in Fig. 3). On the other hand, the magnetospheric component of the luminosity due to rotational energy losses, when the pulsar mechanism is active, would produce very high luminosities at early times for millisecond pulsars (see e.g. Perna & Stella 2004). However, spectral modelling can in principle disentangle the thermal disc component from the power-law emission from the magnetosphere.

When the initial fallback rate is very high, we have already noted (Section 2.2) that, at some epochs, $\Omega_{\rm K} > \Omega$, and the NS is temporarily spun up while accreting. During these transient bright phases, the X-ray brightness of the system is dominated by the accretion luminosity on to the surface of the NS. The exact duration of this transient bright phase and the time at which it sets in are a function of P, $\dot{M}$ and B; a more detailed discussion is beyond the scope of this work. The physical significance of these accretion-powered phases is that if fallback discs around pulsars are ubiquitous, and they set in at high accretion rates, then they would give rise to *a new class of X-ray transients*. Furthermore, we note that a sudden increase in brightness could also occur if, at some point during the evolution, the inner radius switches from $R_{\rm in} < R_{\rm lc}$ to $R_{\rm in} = R_{\rm lc}$, at which point the pulsar mechanism can turn on again.

As already discussed in previous work on fallback discs, the disc is expected to be brighter at wavelengths longer than the X-rays. This is clearly seen by the mid-IR disc luminosity (computed in the 3–4 μm band) also displayed in Fig. 3; the mid-IR luminosity is, especially at later times (when the disc is cooler), substantially larger than the 2–10 keV luminosity (see Perna et al. 2000; Perna & Hernquist 2000, for detailed spectra of fallback discs). Searches for fallback discs in the optical and IR have been numerous, but they have mostly yielded upper limits on the emission. Mignani et al. (2007a,b) derived an upper limit on the K luminosity of the pulsar PSR J1119−6127 of 6.6×10^{30} erg s^{-1}. A dedicated search for fallback discs in four SN remnants was performed by Wang et al. (2007a). Their IR limits are of the order of a few $\times\, 10^{29}$ erg s^{-1} for objects of a few kyr of age. Taken at face value, these limits, once compared with the results of Fig. 3, would imply that fallback discs, if ubiquitous around young NSs, are unlikely to be accreting at very high rates and/or be very large (recall that here we have assumed $R_{\rm out} = 1000\, R_{\rm NS}$). Detection of a fallback disc around an isolated NS was reported by Wang et al. (2006). The mid-IR luminosity was 8.5×10^{31} erg s^{-1} (for a distance of 5 kpc). This value is compatible with our predictions. More generally, IR emission has been detected in a number of isolated NSs (see e.g. Mignani 2011, for a summary). However, lack of a detailed spectral characterization makes it typically difficult to distinguish between magnetospheric and disc emission.

Longer wavelength observations (in the submm) have been reported by Posselt et al. (2010) for the isolated NS RX J1856.5−3754. Using the bolometer array on the Atacama Pathfinder Experiment (APEX) telescope, they determined a flux limit of 5 mJy at 345 GHz. At the estimated distance of 167 pc, this yields a limit of 5.8×10^{28} erg s^{-1} on the luminosity. This value is unconstraining for the discs considered here. And in fact, Posselt et al. (2010) found that it could only set limits on a hypothetical very large outer radius of the disc. The best prospect for detecting the presence of discs around young NSs remains in the optical/IR wavelength range.

3 POPULATION PROPERTIES

3.1 Timing properties

We proceed now to simulate how the ubiquitous presence of fallback discs affects the statistical timing properties of the NS population, for a certain birth spin period and magnetic field distribution. The magnetic field B and the initial disc inflow rate $\dot{M}_0$ are randomly generated according to their respective distributions discussed in Section 2.2. For the initial spin, we consider two distributions: one centred at $P_0 = 5$ ms (representative of fast-born pulsars) and one at $P_0 = 300$ ms (slow-born pulsars); we assume $\sigma_{\log P_0} = 0.2$ for both distributions. Finally, for plotting purposes, we normalize the results to a pulsar birth rate $\dot{N} = 1/100\,{\rm yr}^{-1}$.

In order to simulate the distribution of *observable* radio pulsars, we need to take into account that the radio emission fades with age. Here, we adopt the death probability band empirically defined by Arzoumanian et al. (2002), centred around the line $\dot{P}_{15}/P^3 - 10^{\rm DL_0} = 0$, where P is in seconds, $\dot{P}_{15} \equiv \dot{P}/10^{-15}$ s s^{-1} and $\rm DL_0 = 0.5$. The radio emission can also be disrupted or modified when the disc penetrates the magnetosphere inside the light cylinder (see e.g. Shannon & Cordes 2009, for an extensive discussion). This does not affect the long-term evolution of the period and timing properties computed here. However, if disc penetration inside the magnetosphere were to dim or completely shut down radio emission, then a fraction of pulsars in the sample may not be visible. Previous investigations (e.g. Alpar et al. 2001; Menou et al. 2001a) assumed the inner edge of the disc to be always located at the light cylinder, throughout the entire evolution of the pulsar, so that radio emission would always be ensured. However, when the accretion rate is very high and the ram pressure of the material is larger than the magnetic pressure of the pulsar, there is no compelling reason for imposing that the inner edge of the disc does not penetrate inside the light cylinder. Hence, in this investigation, we let the disc torque operate at its physically expected location, that is the smallest between $R_{\rm m}$ and $R_{\rm lc}$, with the understanding that if $R_{\rm m} < R_{\rm lc}$ the radio signal might be disrupted. With this caveat in mind, in the rest of the paper we conform to the standard language in the literature, and refer to 'dead' pulsars only as to the fraction of pulsars that have passed the death line. For a given distribution of initial parameters, we calculate period distributions for both the full NS population (whether observable or not) and for the subpopulation of observable radio pulsars (before the death-line cut-off).

First, we examine the evolution of pulsar periods for the initial short-period distribution and no death-line cut-off. We show (Fig. 4, left-hand panels) period distributions that include all the pulsars younger than a certain age, for three different ages. The top panel shows the evolution due to the combined effect of disc and dipole radiation loss, while the bottom panel shows, for the same initial parameters, the standard evolution due to dipole losses alone. An interesting and perhaps surprising feature of the evolutionary pattern of the spin distribution in the dipole+disc case is that it becomes bimodal. An inspection of the evolutionary tracks of individual pulsars belonging to each peak shows that the shorter period peak is produced mostly by NSs in which the dipole torque dominates over the disc torque; hence, the timing evolution of those pulsars is only marginally affected by the presence of the disc, at least when the NSs are still relatively young. This can also be seen by comparison with the lower panel, in which we plot the expected evolution in the absence of disc torques. Another (relatively small) contribution to the shorter period peak comes from NSs in the

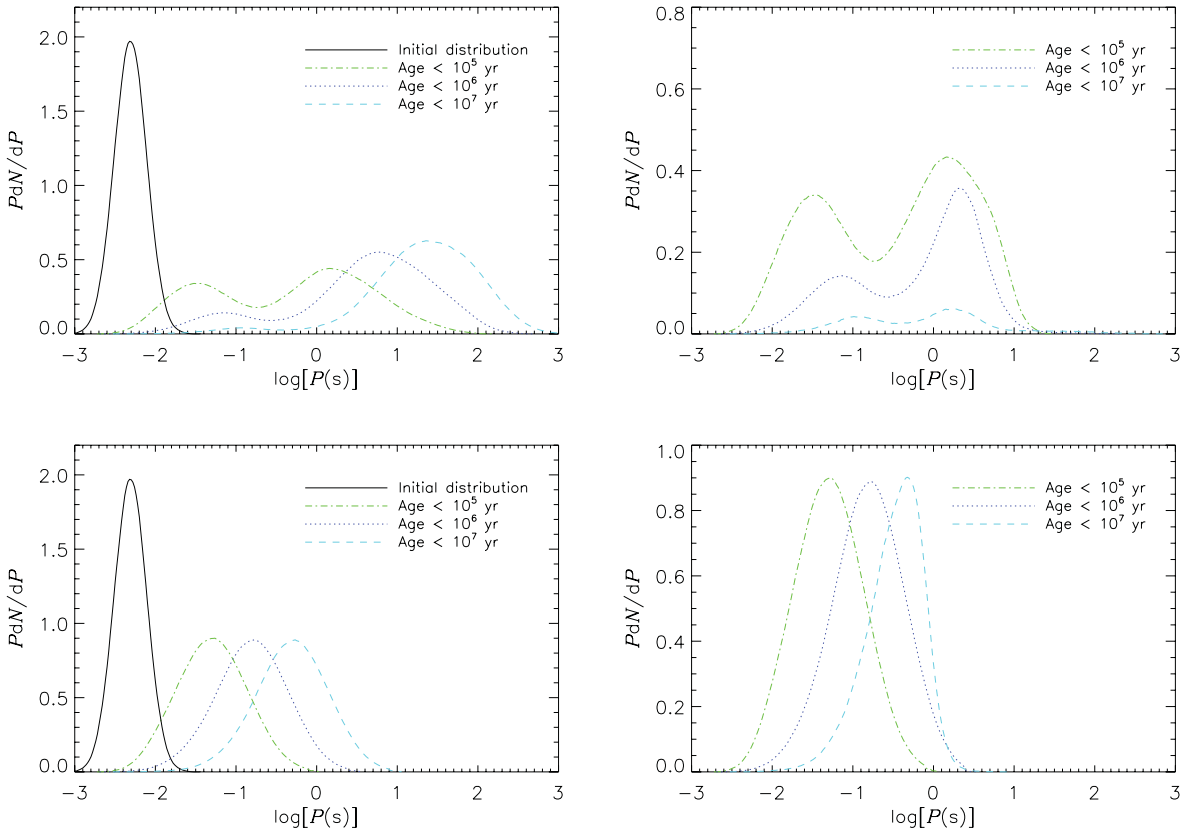

Figure 4. Left: the evolution of a representative, short-period NS spin distribution at birth (solid line) for the case in which the NSs evolve by dipole radiation alone (bottom panel), and for the case in which they evolve as the result of dipole losses together with magnetospheric interaction with a fallback disc (upper panel). Right: same as in the left-hand panels, but including only the pulsars above the death line.

disc-driven spin-up phase, which can bring their spin close to the initial value. The longer period peak of the spin distribution, on the other hand, consists of NSs in which the disc torque dominates. We have seen (Section 2.2) that disc torques are almost always negative: therefore, disc-dominated NSs will more quickly reach longer periods. A similar period bimodality due to disc torques is also apparent in our simulated distribution of observable radio pulsars, before the death line (Fig. 4, right-hand panels).

The observed period distribution of isolated pulsars (ATNF pulsar catalogue: Manchester et al. 2005) is characterized by a dominant broad peak centred around a period of several hundreds milliseconds, and another, much smaller peak, centred around a few milliseconds. If fallback discs are common around isolated NSs, then our results suggest that the millisecond peak might correspond to the small fraction of the NS population which was born with the fastest periods and for which the disc torque was not significant. However, there may also be a contamination from old, weakly magnetized recycled pulsars that were spun up to millisecond periods by disc accretion in a binary system, but have since lost their companion star (e.g. Lorimer et al. 2004).

Our finding that disc accretion leads to a bimodal period distribution is particularly interesting in light of observations of NSs in Be/X-ray binaries, which accrete material at a relatively high rate (from a companion, rather than from fallback). These systems display a bimodal period distribution, with one peak centred around $\sim$10 s and another around $\sim$300 s, previously attributed to two types of SN explosion (Knigge, Coe & Podsiadlowski 2011). We propose instead that high rates of disc accretion and the competing effects of dipole and disc torques may have contributed to this bimodality.

We then repeated our Monte Carlo simulation for the long-period birth distribution. We find that the period distribution remains single peaked at all times (Fig. 5), in marked contrast to the short-period birth case. The reason is that when the initial periods are long, the disc torque dominates over the entire life of the pulsars, for the greatest majority of pulsars.

Fig. 6 shows the distribution of timing ages and braking indices versus real age for the full pulsar distribution; we have also distinguished pulsars above and below the death line. A variable birth rate (higher for the younger objects) has been assumed in order to sample pulsars of different ages more uniformly. The fast-born pulsar distribution shows two clusterings, one at $n \approx 3$ and another at $n \approx 1$: the former from the younger and older pulsars, and the latter for the intermediate phase discussed in Section 2.2. Note how a large fraction of pulsars has $n < 3$, but there can be some very large values. The pulsar distribution with slow initial spins, on the other hand, is largely concentrated in the range $1.5 \lesssim n \lesssim 3$, plus a subset of spinning-up sources found predominantly with $n < 0$. Timing ages are generally smaller than the real ages for the older objects, and larger than the real ages for the younger NSs.

Braking indices have been measured for a number of pulsars. Interestingly, indices smaller than 3 are rather common, and most often with values between 2 and 3 (e.g. Livingstone, Kaspi & Gavriil 2005a; Livingstone et al. 2005b, 2006), with sometimes values smaller than 2 (Lyne et al. 1996). This is the natural range of values predicted by fallback discs, as we have shown.

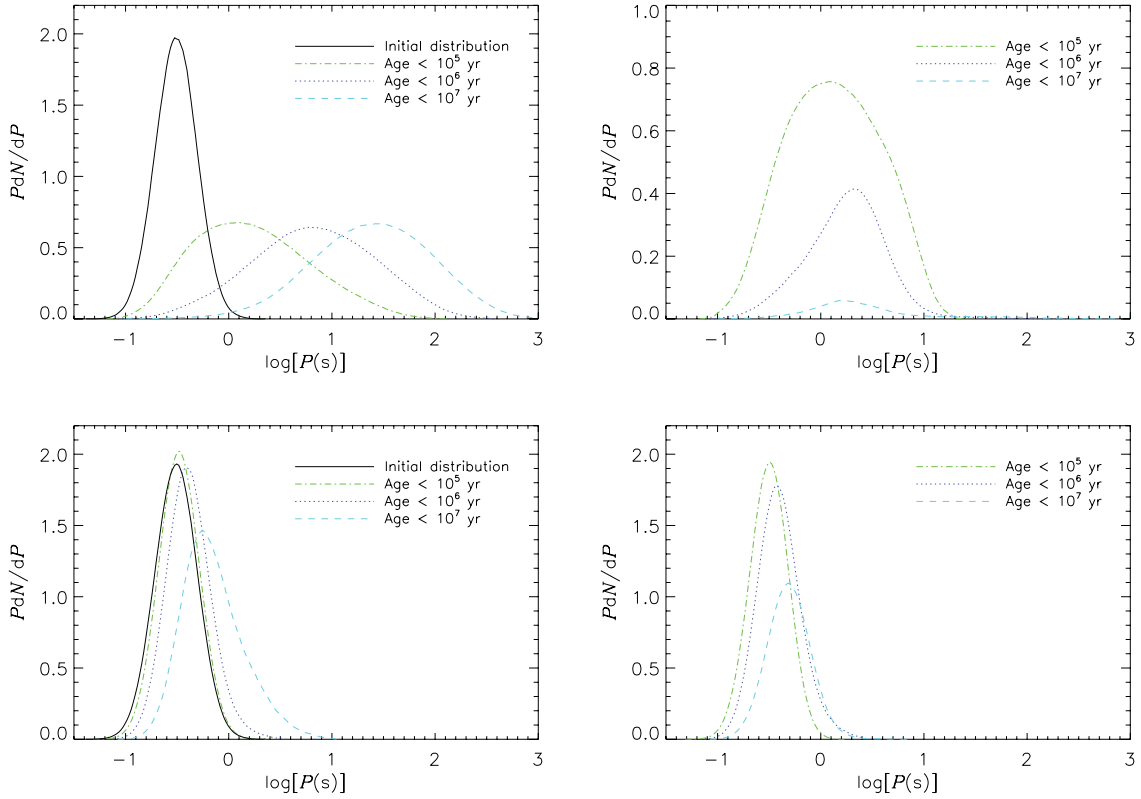

Figure 5. Same as in Fig. 4, but for the long-period spin distribution at birth.

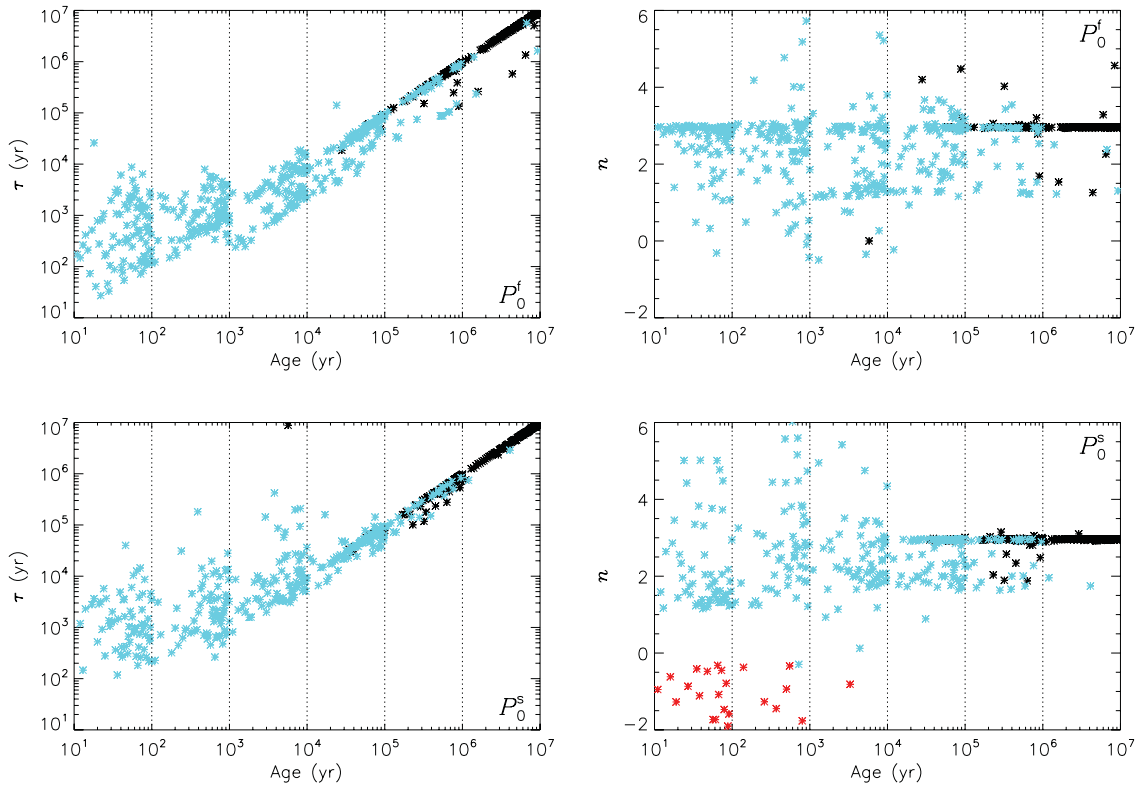

Figure 6. Left-hand panels: simulated timing age distribution for the fast-born (top) and slow-born (bottom) populations in the presence of fallback discs. NSs above the death line are plotted in cyan, and those beyond the death line in black. The birth rate is a function of age bin, in order to have the same number of data points in every log bin (namely, a rate of 1 yr^{-1} for $10 <$ age $< 10^2$ yr, 1/10 yr^{-1} for $10^2 <$ age $< 10^3$ yr, etc.). Right-hand panels: same as in the left-hand panels, but for the braking index distribution. NSs that are spinning up are plotted in red.

3.2 Luminosity properties

We have seen in Section 2.1 that the initial inflow rate from a fallback disc can be much larger than the critical value at large radii, and the emitted bolometric luminosity can exceed the Eddington limit by a logarithmic factor. In our model, during this initial phase, the mass inflow at large radii declines as $(t/t_0)^{-19/16}$, and most of the inflow is lost in a wind when $\dot{M}_{\rm out} > \dot{M}_{\rm Edd}$. We have also shown that the decay time-scale is $t_0 \sim 10^2$–10^4 s for typical disc parameters. Thus, the supercritical phase of accretion has a very short duration. The rapid decline in the disc luminosity is due to the combined effect of the decline in the accretion rate and the increase of the magnetospheric radius, which defines the inner truncation radius of the disc. Note that the disc luminosity in the X-ray band, being produced in the inner parts of the disc, is especially sensitive not only to the magnitude of the accretion rate, but also to the spin period of the NS. The reason lies in the fact that the inner radius of the disc, $R_{\rm in}$, being determined by the minimum between $R_{\rm m}$ and $R_{\rm lc}$, depends on both $\dot{M}$ (through $R_{\rm m}$) and Ω (through $R_{\rm lc}$). The longer wavelength emission, on the other hand, being produced at larger disc radii, is less sensitive to the precise location of the inner radius, and hence it has also little sensitivity on the spin period of the NS.

The characteristic peak disc temperature is

$$T_{\rm in} \approx \left(\frac{3GM\dot{M}}{8\pi\sigma\, R_{\rm in}^3}\right)^{1/4} \approx \begin{cases} 0.96\times10^6\, M_{\rm NS,1}^{5/14}\, B_{12}^{-3/7}\, \dot{M}_{18}^{13/28}\ {\rm K} \\ \qquad\qquad\qquad\qquad \text{for } R_{\rm in} = R_{\rm m} \\ 1.27\times10^6\, M_{\rm NS,1}^{1/4}\, \dot{M}_{18}^{1/4}\, P_{10\,{\rm ms}}^{-3/4}\ {\rm K} \\ \qquad\qquad\qquad\qquad \text{for } R_{\rm in} = R_{\rm lc}. \end{cases} \quad (17)$$

With our chosen range of initial inflow rates, we find that the peak temperature is $\approx 10^6$ K ≈ 0.1 keV for an initial period of time lasting $\sim 10^2$–10^4 yr, and then declines $\sim t^{-0.55}$ afterwards. Thus, fallback discs are always much cooler than accretion discs in NS X-ray binaries, even when they are both near the Eddington luminosity. This is because the magnetic field of an old NS in an X-ray binary is generally weaker than in a young pulsar,[3] and the disc can extend closer to the innermost stable circular orbit or the NS surface, reaching peak temperatures $\sim$1–2 keV. This is also the reason why disc accretion tends to spin down young pulsars and spin up old pulsars. In summary, we expect the direct luminosity effect of a fallback disc to be a supersoft component in addition to the thermal component from the NS surface. A noteworthy result of our analysis is that at early times, $t \lesssim 10^3$–10^4 yr, the 0.1–10 keV luminosity from the disc is expected to exceed the luminosity from the NS surface for the range of initial accretion rates considered here, $\dot{M}(t=0) \gtrsim 10^{25}\,{\rm g\,s^{-1}}$. This is especially so for millisecond pulsars, since at early times $R_{\rm in} = R_{\rm lc}$, and hence the inner radius of the disc is smaller for shorter period NSs. Lack of detection of this disc component in young NSs would argue against a ubiquitous formation of fallback discs, or that the initial accretion rates are lower than what numerical simulations suggest. In millisecond pulsars, discs could be blown away by the pulsars themselves (Ekşi et al. 2005).

Lastly, to conclude our discussion of the luminosity, note that when the non-thermal magnetospheric component is enabled, it would likely dominate in the 2–10 keV band at least for the fastest pulsars. In this case, our model suggests that the X-ray colours and spectral appearance of a young pulsar with a fallback disc truncated at the magnetospheric radius would be somewhat similar to those observed in the largest class of ultraluminous X-ray sources (see Feng & Soria 2011, for a review), dominated by a power-law component of photon index $\approx$2, with a soft excess at $kT \approx 0.1$–0.2 keV and possibly a radiation-driven disc outflow. This is likely to be a coincidence due to the relative scaling of accretor mass, accretion rate in Eddington units and characteristic inner disc radius in the two classes of objects. If the thermal component of the luminosity in both classes of objects is Eddington limited, young pulsars with fallback discs will be one or two orders of magnitude less luminous than ultraluminous X-ray sources with cool discs, and there would not be possibility of misidentification if the distance is known. Another main difference is that the X-ray luminous phase of a fallback disc lasts only $\lesssim 10^4$ yr, which implies that such sources must be found very close to their natal SN remnant; instead, ultraluminous X-ray sources are thought to be active for $\gtrsim 10^6$ yr and they are very rarely associated with SN remnants. Moreover, the characteristic inner radius of the standard disc in power-law-dominated ultraluminous X-ray sources tends to increase with the accretion rate (for example, $R_{\rm in} \sim \dot{M}$ if it corresponds to the spherization radius) in the supercritical regime; as a result, the thermal component becomes cooler but more luminous (Soria 2007; Kajava & Poutanen 2009). Instead, the inner radius of a disc truncated at the magnetospheric boundary will be pushed outwards as the accretion rate declines (assuming that the NS magnetic field varies more slowly than the accretion rate): $R_{\rm m} \sim \dot{M}^{-2/7}$, implying $T_{\rm in} \sim \dot{M}^{13/28} \sim t^{-0.55}$ and $L_{\rm bol} \sim T_{\rm in}^{36/13} \sim t^{-1.52}$. At late times, the disc becomes too faint and cool to be detectable in the X-ray band. Then the best prospects for direct detection are at longer wavelengths, especially in the IR.

4 SUMMARY AND CONCLUSIONS

Fallback discs have been suggested to be a common outcome of SN explosions. In this paper, we have explored some of the consequences of their presence for the timing and spectral properties of the associated NS population. To this purpose, we have modelled the torque and luminosity of fallback discs around young pulsars, with a range of values for the initial spin and dipole magnetic field. Relying on the results of numerical simulations of massive star collapse, we assumed that the initial inflow rate of fallback material at large radii is highly supercritical, but most of the inflow is blown away in a radiatively driven wind, so that the accretion rate at the inner edge of the disc is Eddington limited.

We considered two initial distributions of spin periods: one with a Gaussian distribution centred at 5 ms and one centred at 300 ms, with a birth rate proportional to the star formation rate (assumed constant). We evolved the period distribution of the two populations over time, under the combined effect of dipole and fallback disc torques. The main outcomes of our analysis are summarized below.

(i) We find that, within the wide range of initial parameters explored, the effect of a fallback disc is mostly a spin-down. Matter

[3] The issue of magnetic field decay (Goldreich & Reisenegger 1992) is still not fully settled as far as its quantitative details are concern. However, observations (see e.g. summary in Zhang 2007) suggest that both atoll and Z sources (the two classes of low-mass X-ray binaries) have weaker B fields; this observational evidence is based on the X-ray spectra, the luminosity at which they switch from propeller to accretor, and also on the existence of recycled millisecond pulsars, which could not be spun up to millisecond periods if they had a high magnetic field.

from the disc is propelled out rather than being accreted on the NS surface, except for a few short phases when the accretion rate is very high. During these phases, which can last up to several thousand years, the NS–disc system brightens up in X-rays to a luminosity that can reach the Eddington value, and the NS is spun up to levels that can bring the spin close to its initial value.

(ii) If fallback discs are common, they substantially affect our estimates of the initial spin birth of pulsars (which generally assume spin-down losses due to dipole radiation alone). In particular, the period distribution of fast-born pulsars is predicted to evolve towards a bimodal distribution, unlike the distribution in the absence of fallback discs, which remains single peaked if it started as such. On the other hand, for slow-born pulsars, the main long-term effect is simply a shift of the distribution to longer periods.

(iii) Timing ages as measured for the NS/disc system generally overestimate real ages for young pulsars, and underestimate it for old pulsars. Braking indices cluster in the range $1.5 \lesssim n \lesssim 3$ for slow-born pulsars (apart from a short-lived spin-up phase with $-0.5 \lesssim n \lesssim -2$) and $-0.5 \lesssim n \lesssim 5$ for fast-born pulsars. Younger objects tend to have $n \lesssim 3$. Large values of n, while not common, are possible, and associated with phase transitions in the pulsar–disc system.

(iv) In addition to changing the spin evolution of a pulsar (and therefore also its rotation-powered X-ray luminosity), a fallback disc can be directly detected as a bright source in a broad wavelength range. We found that at early times the characteristic inner disc temperature $kT_{\rm in} \sim 0.1$ keV for typical initial values of the magnetic field, $B \sim 10^{12}$ G, and Eddington-limited accretion, and declines as $T_{\rm in} \sim \dot{M}^{13/28} \sim t^{-0.55}$ at later epochs. The disc has a low temperature compared with typical accretion discs in (older) NS X-ray binaries, because it is truncated at the magnetospheric radius. The 0.1–10 keV luminosity generally exceeds that of the NS surface at early times if the initial accretion rates are highly super-Eddington. Lack of detection of such a soft X-ray excess in young objects can help put constraints on the ubiquity of fallback discs.

ACKNOWLEDGMENTS

RS acknowledges support from a Curtin University Senior Research Fellowship, and hospitality at the Mullard Space Science Laboratory (UK) and at the University of Sydney (Australia) during part of this work. This work was partially supported by grants NSF AST-1009396, AR1-12003X and DD1-12053X (RP). We thank an anonymous referee for very insightful comments which greatly helped the presentation of our work.

REFERENCES

Abramowicz M. A., Czerny B., Lasota J. P., Szuszkiewicz E., 1988, ApJ, 332, 646
Alpar M. A., 2001, ApJ, 554, 1245
Alpar M. A., Ankay A., Yazgan E., 2001, ApJ, 557, L61
Arzoumanian Z., Chernoff D. F., Cordes J. M., 2002, ApJ, 568, 289
Bildsten L. et al., 1997, ApJS, 113, 367
Blackman E. G., Perna R., 2004, ApJ, 601, L71
Blaes O., Madau P., 1993, ApJ, 403, 690
Blaschke D., Grigorian H., Voskresensky D. N., 2004, A&A, 424, 979
Bondi H., 1952, MNRAS, 112, 195
Cannizzo J. K., Lee H. M., Goodman J., 1990, ApJ, 351, 38
Chatterjee P., Hernquist L., 2000, ApJ, 543, 368
Chatterjee P., Hernquist L., Narayan R., 2000, ApJ, 534, 373
Chevalier R. A., 1989, ApJ, 346, 847
Coe M. J., Pightling S. L., 1998, MNRAS, 299, 223
Cumming A., Zweibel E., Bildsten L., 2001, ApJ, 557, 958
Ekşi K. Y., Hernquist L., Narayan R., 2005, ApJ, 623, L41
Faucher-Giguère C.-A., Kaspi V. M., 2006, ApJ, 643, 332
Feng H., Soria R., 2011, New Astron. Rev., 55, 166
Frank J., King A. R., Raine D. J., 2002, Accretion Power in Astrophysics. Cambridge Univ. Press, Cambridge
Geppert U., Page D., Zannias T., 1999, A&A, 345, 847
Goldreich P., Reisenegger A., 1992, ApJ, 395, 240
Gunn J. E., Ostriker J. P., 1970, ApJ, 160, 979
Hulleman F., van Kerkwijk M. H., Verbunt F. W. M., Kulkarni S. R., 2000a, A&A, 358, 605
Hulleman F., van Kerkwijk M. H., Kulkarni S. R., 2000b, Nat, 408, 689
Illarionov A. F., Sunyaev R. A., 1975, A&A, 39, 185
Israel G. L. et al., 2003, ApJ, 589, L93
Kajava J. J. E., Poutanen J., 2009, MNRAS, 398, 1450
Kaplan D. L., Kulkarni S. R., Murray S. S., 2001, ApJ, 558, 270
Kaplan D. L., Chakrabarty D., Wang Z., Wachter S., 2009, ApJ, 700, 149
Kargaltsev O., Pavlov G. G., 2008, in Bassa C., Wang Z., Cumming A., Kaspi V. M., eds, AIP Conf. Ser. Vol. 983, 40 Years of Pulsars: Millisecond Pulsars, Magnetars and More. Am. Inst. Phys., New York, p. 171
Knigge C., Coe M., Podsiadlowski P., 2011, Nat, 479, 372
Kuncic Z., Bicknell G. V., 2007, Ap&SS, 311, 127
Liu X.-W., Li X.-D., 2009, ApJ, 692, 723
Livingstone M. A., Kaspi V. M., Gavriil F. P., 2005a, ApJ, 633, 1095
Livingstone M. A., Kaspi V. M., Gavriil F. P., Manchester R. N., 2005b, ApJ, 619, 1046
Livingstone M. A., Kaspi V. M., Gotthelf E. V., Kuiper L., 2006, ApJ, 647, 1286
Lorimer D. R. et al., 2004, MNRAS, 347, L21
Lyne A. G., Manchester R. N., Taylor J. H., 1985, MNRAS, 213, 613
Lyne A. G., Pritchard R. S., Graham-Smith F., Camilo F., 1996, Nat, 381, 497
MacFadyen A. I., Woosley S. E., Heger A., 2001, ApJ, 550, 410
Manchester R. N., Hobbs G. B., Teoh A., Hobbs M., 2005, AJ, 129, 1993
Marsden D., Lingenfelter R. E., Rothschild R. E., 2001a, ApJ, 547, L45
Marsden D., Lingenfelter R. E., Rothschild R. E., Higdon J. C., 2001b, ApJ, 550, 397
Menou K., Esin A. A., Narayan R., Garcia M. R., Lasota J.-P., McClintock J. E., 1999, ApJ, 520, 276
Menou K., Perna R., Hernquist L., 2001a, ApJ, 554, L63
Menou K., Perna R., Hernquist L., 2001b, ApJ, 559, 1032
Michel F. C., 1988, Nat, 333, 644
Mignani R. P., 2011, Advances Space Res., 47, 1281
Mignani R. P. et al., 2007a, Ap&SS, 308, 203
Mignani R. P., Perna R., Rea N., Israel G. L., Mereghetti S., Lo Curto G., 2007b, A&A, 471, 265
Mineshige S., Nomura H., Hirose M., Nomoto K., Suzuki T., 1997, ApJ, 489, 227
Narayan R., Ostriker J. P., 1990, ApJ, 352, 222
Ohsuga K., Mineshige S., 2011, ApJ, 736, 2
Perna R., Hernquist L., 2000, ApJ, 544, L57
Perna R., MacFadyen A., 2010, ApJ, 710, L103
Perna R., Stella L., 2004, ApJ, 615, 222
Perna R., Hernquist L., Narayan R., 2000, ApJ, 541, 344
Perna R., Narayan R., Rybicki G., Stella L., Treves A., 2003, ApJ, 594, 936
Perna R., Bozzo E., Stella L., 2006, ApJ, 639, 363
Perna R., Soria R., Pooley D., Stella L., 2008, MNRAS, 384, 1638
Phinney E. S., Blandford R. D., 1981, MNRAS, 194, 137
Popov S. B., Colpi M., Treves A., Turolla R., Lipunov V. M., Prokhorov M. E., 2000, ApJ, 530, 896
Posselt B., Schreyer K., Perna R., Sommer M. W., Klein B., Slane P., 2010, MNRAS, 405, 1840
Possenti A., Cerutti R., Colpi M., Mereghetti S., 2002, A&A, 387, 993
Poutanen J., Lipunova G., Fabrika S., Butkevich A. G., Abolmasov P., 2007, MNRAS, 377, 1187
Saito Y., Kawai N., Kamae T., Shibata S., Dotani T., Kulkarni S. R., 1997, ApJ, 477, L37
Shakura N. I., Sunyaev R. A., 1973, A&A, 24, 337

Shannon R. M., Cordes J. M., 2009, ApJ, 682, 1152
Shibazaki N., Murakami T., Shaham J., Nomoto K., 1989, Nat, 342, 656
Soria R., 2007, Ap&SS, 311, 213
Srinivasan G., Dwarakanath K. S., Bhattacharya D., 1984, J. Astrophys. Astron., 5, 403
Vrtilek S. D., Raymond J. C., Garcia M. R., Verbunt F., Hasinger G., Kurster M., 1990, A&A, 235, 162
Wang Z., Chakrabarty D., Kaplan D. L., 2006, Nat, 440, 772
Wang Z., Kaplan D. L., Chakrabarty D., 2007a, ApJ, 655, 261
Wang Z., Kaspi V. M., Higdon S. J. U., 2007b, ApJ, 665, 1292
Watarai K.-Y., Fukue J., Takeuchi M., Mineshige S., 2000, PASJ, 52, 133
Zampieri L., Turolla R., Zane S., Treves A., 1995, ApJ, 439, 849
Zhang C. M., 2007, in Einstein's, ESO Astrophys. Symp., Relativistic Astrophysics Legacy and Cosmology. Springer-Verlag, Berlin, p. 490
Zhang W., Woosley S. E., Heger A., 2008, ApJ, 679, 639

This paper has been typeset from a TEX/LATEX file prepared by the author.